Available online at www.sciencedirect.com
ScienceDirect
Journal of Solid State Chemistry 180 (2007) 3166–3171
JOURNAL OF SOLID STATE CHEMISTRY
www.elsevier.com/locate/jssc

Crystal structure of $Ca_2Ln_3Sb_3O_{14}$ (Ln = La, Pr, Nd and Y): A novel variant of weberite

Y.S. Au, W.T. Fu, D.J.W. IJdo*

Leiden Institute of Chemistry, Gorlaeus Laboratories, Leiden University, P.O. Box 9502, 2300 RA Leiden, The Netherlands

Received 20 July 2007; received in revised form 6 September 2007; accepted 8 September 2007
Available online 20 September 2007

Abstract

The crystal structures of $Ca_2Ln_3Sb_3O_{14}$ (Ln = La, Pr, Nd and Y) and $Ca_2Sb_2O_7$ at room temperature were refined by the Rietveld method using combined X-ray and neutron powder diffraction data. $Ca_2Sb_2O_7$ adopts the weberite structure having the space group *Imma*. The structures of $Ca_2Ln_3Sb_3O_{14}$ are, however, neither the orthorhombic nor the tetragonal chiolite as has been suggested previously. They crystallize in the monoclinic space group $I2/m11$ belonging to a hitherto unknown type of deformation of the parent (orthorhombic) weberite structure.

Keywords: Weberites; X-ray powder diffraction; Neutron powder diffraction; Crystal structure

1. Introduction

In oxides of the stoichiometry $A_2Sb_2O_7$, two structures have been found previously: the orthorhombic weberite (Na_2MgAlF_7) and the cubic pyrochlore [1]. The phases occurring in the system $A_2Sb_2O_7$ as a function of A-cations and the adoption of either the weberite or the pyrochlore structure have been studied in detail by Knop et al. [2]. For example, $Ca_2Sb_2O_7$ occurs in both the weberite and the pyrochlore form depending on the pressure applied during the synthesis. High pressure favours the pyrochlore structure. On the other hand, $Sr_2Sb_2O_7$ is found to crystallize only in the weberite form. $Pb_2Sb_2O_7$ has the pyrochlore structure at room temperature and transforms to the weberite structure above 510 K [3].

The weberite structure has the space group *Imma*, in which half of the SbO_6 octahedra are linked to neighbouring SbO_6 units through all of their vertices; the other half is connected through four vertices only. All oxygen anions are part of the octahedral framework, which results in the weberite Sb_2O_7 stoichiometry. The two different A-cations are coordinated to eight oxygens: one is in a square prism and the other is in a hexagonal bipyramid. The pyrochlore structure ($Fd\bar{3}m$), e.g. $Pb_2Sb_2O_7$, is derived from an anion-deficient fluorite structure. All SbO_6 octahedra share each oxygen with one other group so that the composition of the framework is actually $Sb_2O_6^{2-}$. One oxygen atom, O at 8*b* is not part of the SbO_6 framework; it coordinates to atoms of type A only. The A-cations have 8 coordination to oxygen.

A related structure is the chiolite-type ($Na_5Al_3F_{14}$) (4). Again all fluoride ions belong to the AlF_6 octahedral framework. The structure consists of layers of composition Al_3F_{14}, in which one-third of the AlF_6 octahedra share four corners, the other two-thirds share two corners with neighbouring AlF_6 groups only. The space group for the ideal chiolite is $I4/mmm$, but $Na_5Al_3F_{14}$ crystallizes in the subgroup $P4/mnc$ [4]. Oxides with the chiolite structure of lower symmetry are known for $Sr_5U_3O_{14}$ and $BaSr_4U_3O_{14}$ [5]. The positions of the larger cations in weberite and chiolite are strongly related.

A number of oxides of the formula $A_2B_2O_7$ are known to have the weberite structure. Examples are $A_2Sb_2O_7$ (A = Ca, Sr, and Pb) [2,3,6], $Ca_2Os_2O_7$ [7], $Ba_2U_2O_7$ [8] and $Na_2Te_2O_7$ [9]. Substitution of different cations in weberites is possible. For example, $SrCdSb_2O_7$ [10], $NaLnSb_2O_7$ (Ln = lanthanides) [11,12] and $NaA_3FeTe_3O_{14}$

*Corresponding author. Fax: +31 71 5274537.
E-mail address: d.ijdo@chem.leidenuniv.nl (D.J.W. IJdo).

0022-4596/$ - see front matter © 2007 Published by Elsevier Inc.
doi:10.1016/j.jssc.2007.09.013

(A=Ca, Cd) [12] have been reported to adopt the weberite structure; but the structural details are not yet known. The compounds $Ca_2Ln_3Sb_3O_{14}$ [13], with Ln = La, Nd, Sm and Gd, have been reported to be orthorhombically distorted chiolite. For smaller lanthanides, i.e. Ln = Dy, Yb, Lu and Y, the tetragonal chiolite structure with space group $P4/mnc$ was proposed [13].

There is currently some interest in the photo-catalytic properties of weberite-like compounds. It has been shown that antimonates $M_2Sb_2O_7$ with M = Sr and Ca are active photo-catalysts for water decomposition if they are loaded with RuO_2 [14]. $M_2Sb_2O_7$ are also known to be photo-catalytically active for degrading methyl orange under UV light. Interestingly, the catalytic efficiency of $Sr_2Sb_2O_7$ is much higher than that of $Ca_2Sb_2O_7$ [15]. In relation to our earlier work on the chiolite-like structures, e.g. $BaSr_4U_3O_{14}$ and $Sr_5U_3O_{14}$ [5], we have investigated the structures of $Ca_2Ln_3Sb_3O_{14}$, Ln = La, Pr, Nd and Y, using the combination of neutron powder diffraction and X-ray powder diffraction data. For the purpose of comparison, the structure of $Ca_2Sb_2O_7$ was also refined as some uncertainties concerning the space group and the oxygen parameters are still persisting [9,16]. In this paper, we describe the crystal structures of both $Ca_2Sb_2O_7$ and $Ca_2Ln_3Sb_3O_{14}$. The former is confirmed to be weberite; the later compounds crystallize in the space group $I2/m11$ belonging to a new monoclinic deformation of the weberite-type structure.

2. Experimental

Samples of $Ca_2Ln_3Sb_3O_{14}$ were prepared by the standard solid-state reaction from the appropriate mixtures of $CaCO_3$, Ln_2O_3, Pr_6O_{11}, Tb_4O_7 and Sb_2O_3 in alumina crucibles. The thoroughly ground mixtures were first heated in air at 600 °C over night and, then, at 1350 °C for several days with repeated grindings. After the last firing the samples were furnace cooled to room temperature.

X-ray powder diffraction data were recorded using a Philips X'Pert diffractometer, equipped with the X'Celerator using Cu$K\alpha$ radiation, in steps of 0.02° (2θ) and 8 s counting time between 10° and 140° (2θ). Neutron powder diffraction data were collected on the powder diffractometer of the Petten High Flux Reactor. A wavelength of 1.4317 Å was used for Ln = La, Pr, Nd and Y. For $Ca_2Sb_2O_7$ the neutron wavelength used is 2.5718 Å. The calculations were performed using the Rietica computer program [17]. A polynomial function with six parameters was used to fit the background. The profiles have been fitted using a pseudo-Voight function for X-ray and a Gauss function for neutrons.

3. Results

X-ray powder diffraction of $Ca_2Ln_3Sb_3O_{14}$ has shown similar patterns indicating that they are probably isostructural. It was found that the preparation of very pure phases for some lanthanides is difficult: traces of the double perovskite phase Ca_2LnSbO_6 showed up in the X-ray patterns. This is particularly the case when the size of lanthanide becomes relatively small, which is possibly due to the sluggish reactivity or the increased stability of the perovskite-like structure.

The structure of $Ca_2Sb_2O_7$ was refined using the structure of $Sr_2Sb_2O_7$ [6] as a trial model. The refinement, using the neutron powder diffraction data and the space group $Imma$ went quite smoothly. After convergence, the agreement factor (R_{wp}) drops to 3.53%, indicating that the model is appropriate. As was mentioned above, Burchard and Rüdorff [13] have found, based on X-ray powder diffraction data, a body-centred orthorhombic unit cell for $Ca_2Ln_3Sb_3O_{14}$ containing larger lanthanides, e.g. Ln = La, Nd, Sm and Gd [12]. The authors suggested that these compounds crystallize in a (deformed) chiolite structure; however, they did not define the model. For $Ca_2Ln_3Sb_3O_{14}$ with smaller Ln, i.e. Dy, Yb, Lu and Y, they reported a tetragonal cell, and modelled the structure with that of chiolite ($Na_5Al_3F_{14}$) in the space group $P4/mnc$. In their model, part of Ca was allocated to the 2a position; the remaining Ca and Ln were randomly distributed over the 8g position. Using this model, the strong reflections of the X-ray diffraction pattern could be fitted reasonably well as was noted also by the above-mentioned authors; but the fit to the neutron diffraction data, especially in the case of $Ca_2Y_3Sb_3O_{14}$, was very poor. Attempting to use other trial models derived from the chiolite structure was also unsuccessful. Considering that the lattice parameters of $Ca_2La_3Sb_3O_{14}$ reported by Burchard and Rüdorff [13] resemble those observed in $Ca_2Sb_2O_7$ and $Sr_2Sb_2O_7$, we thought that the structure of $Ca_2Ln_3Sb_3O_{14}$ may actually be of the weberite-type. However, the orthorhombic model used for $Ca_2Sb_2O_7$ was found to be unsuitable: refinements using either neutron or X-ray powder diffraction data showed quite large discrepancies. Therefore, in the new model we considered the difference in stoichiometry of the title compounds with the parent weberite structure; one of the four Sb has to be replaced. To conserve the typical feature of the weberite structure, i.e. rows of corner-linked SbO_6 octahedra in the [100] direction, as well as the observed I-centering, the space group $I2/m11$*, a subgroup of $Imma$, was chosen. This space group allows splitting up of some atomic positions compared to the parent weberite structure. Taking into account the chemical composition, the Ca and Ln ions are distributed partly randomly in the metal positions (see also Section 4). Considering further that neutron powder diffraction is more sensitive to the oxygen positions and X-ray diffraction provides better information on the symmetry as well as the cation ordering, the structures of $Ca_2Ln_3Sb_3O_{14}$ with Ln = La, Pr, Nd and Y were refined from the combined neutron and X-ray powder diffraction data [18].

*For ease of comparison with the parent structure, the non-standard space group $I2/m11$ was used in the refinement.

The Rietveld refinement yielded good agreement between the experimental and calculated data. In particular, the model also fits the members with smaller lanthanides nicely, e.g. $Ca_2Y_3Sb_3O_{14}$, which have been described earlier as primitive tetragonal structures. Fig. 1 shows the plots of the observed and calculated neutron profiles of $Ca_2Sb_2O_7$ and two representatives of $Ca_2Ln_3Sb_3O_{14}$ with $Ln = La$ and Y. The refined lattice parameters and the atomic positions are given in Table 1. Some selected interatomic distances and angles are listed in Table 2.

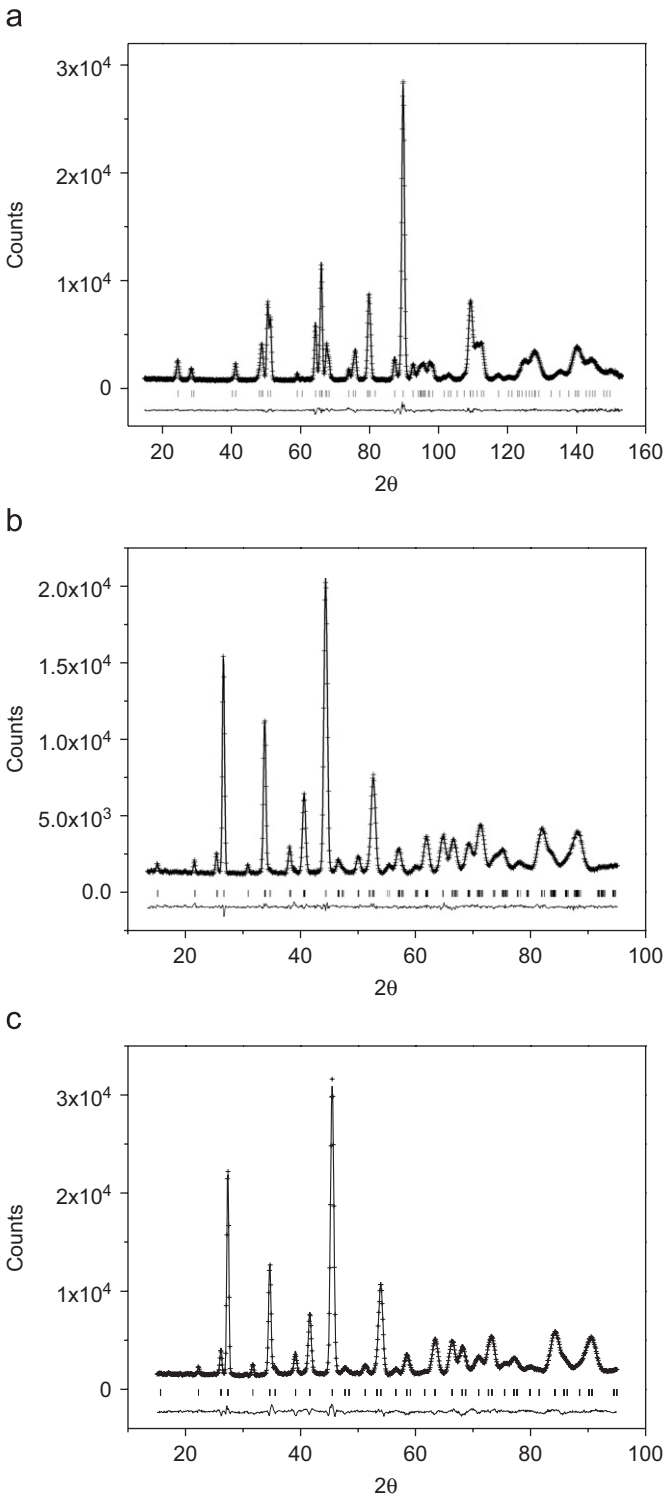

Fig. 1. Observed (crosses) and calculated (full line) profiles of the neutron powder diffraction for $Ca_2Sb_2O_6$ (a) and $Ca_2Ln_3Sb_3O_{14}$ (Ln = La and Y) (b and c), respectively. Tick marks below the profiles indicate the positions of the allowed Bragg reflections. A difference curve (observed–calculated) is shown at the bottom of each plot. Note that the neutron wavelengths used are 2.5718 Å for $Ca_2Sb_2O_6$ and 1.4317 Å for $Ca_2Ln_3Sb_3O_{14}$.

4. Discussion

4.1. $Ca_2Sb_2O_7$

The present investigation is in agreement with the earlier work of Byström [16] who determined approximate positions of the oxygen atoms in this compound. The structure of $Ca_2Sb_2O_7$ consists of rows of corner-linked $Sb(1)O_6$ octahedra along the [100] direction. The octahedra are tilted around an axis parallel to the *b*-axis (Fig. 2). Between the octahedra lie the rows of $Ca(2)O_8$ square prisms, linked by common edges and by two edges of the $Sb(1)O_6$ octahedra, forming slabs perpendicular to the [010] direction. The $Sb(2)O_6$ octahedra lie between the slabs sharing four corners with the $Sb(1)O_6$ octahedra, two corners with $Ca(2)O_8$ square prisms and common edges with $Ca(1)O_8$ hexagonal bipyramids. The latter share also four edges with $Sb(1)O_6$ octahedra. The oxygen atoms are all coordinated by four cations: O(1) and O(3) by two Sb and two Ca and O(2) by one Sb and three Ca.

In the past, there has been some discussion about the true space group of the mineral weberite (Na_2MgAlF_7). Byström [19] originally determined the structure to be in *Imm*2; but the existence of very weak reflections (*hk*0) with $h = 2n+1$ might originate from multiple scattering due to the Renninger effect [20]. To see whether the space group *Imm*2 better describes the structure of $Ca_2Sb_2O_7$, we carried out an additional refinement. However, the *Imm*2 model did not result in any appreciable improvement. In fact, the agreement factors obtained are even slightly higher than those obtained by using the *Imma* model. We concluded that the space group *Imma* is consistent with our neutron powder diffraction data and correctly describes the structure of $Ca_2Sb_2O_7$.

4.2. $Ca_2LnSb_3O_{14}$

The structure of $Ca_2La_3Sb_3O_{14}$ ($Z = 2$) is derived from that of $Ca_2Sb_2O_7$ ($Z = 4$) by substitution of two Ca and one Sb with three La. Replacing Ca1 at $(0,\frac{1}{2},0)$ and $(\frac{1}{2},0,\frac{1}{2})$ and Sb2 at $(0,\frac{1}{2},\frac{1}{2})$ and $(\frac{1}{2},0,0)$ by Ca and La at random lowers the symmetry to $I\bar{2}/m11$. La is also present at four-fold $(\frac{1}{4},\frac{1}{4},\frac{3}{4})$ positions. Consequently, $Ca_2La_3Sb_3O_{14}$ is a deformed weberite. Being similar to $Ca_2Sb_2O_7$, the structure consists of rows of the corner-linked $Sb(1)O_6$ octahedra along the [100] direction (Fig. 2), tilted around the axes parallel to the [010] and [001] direction. The tilting of $Sb(1)O_6$ around [010] is smaller (3.2°) than the tilting in $Ca_2Sb_2O_7$ (21.4°). On the other hand, the tilting parallel to

Table 1
Refined lattice parameters, atomic positions and thermal parameters of $Ca_2Ln_3Sb_3O_{14}$ (*Ln* = La, Pr, Nd and Y) and $Ca_2Sb_2O_7$ in the space groups *I*2/*m*11 and *Imma*, respectively

	$Ca_2La_3Sb_3O_{14}$	$Ca_2Pr_3Sb_3O_{14}$	$Ca_2Nd_3Sb_3O_{14}$	$Ca_2Y_3Sb_3O_{14}$		$Ca_2Sb_2O_7$
S.G.	*I*2/*m*11					*Imma*
a (Å)	7.5753(3)	7.5188(3)	7.5019(2)	7.3905(1)		7.30119(9)
b (Å)	10.6870(5)	10.6111(4)	10.5890(3)	10.4563(2)		10.2147(1)
c (Å)	7.5482(3)	7.4952(2)	7.4770(2)	7.3894(1)		7.46574(9)
α (deg.)	90.346(3)	90.315(2)	90.298(2)	90.049(1)		
V (Å^3)	611.07(5)	597.99(4)	593.94(3)	571.04(2)		556.79(1)
Ca1	2*a*(0,0,0)			(Ca,Y)1[b]	Ca1	4*a*(0,0,0)
Ca11/*Ln*11[a]	2*c*(0,$\frac{1}{2}$,0)			(Ca11/Y11)[b]	*B* (Å)^2	0.66(5)
*Ln*2	4*f*($\frac{1}{4}$,$\frac{1}{4}$,$\frac{3}{4}$)			(Ca2/Y2)[b]	Ca2	4*d*($\frac{1}{4}$,$\frac{1}{4}$,$\frac{3}{4}$)
Ca22/*Ln*22[a]	2*b*(0,$\frac{1}{2}$,$\frac{1}{2}$)			(Ca22/Y22)[b]	*B* (Å)^2	0.97(6)
Sb1	4*e*($\frac{1}{4}$,$\frac{1}{4}$,$\frac{1}{4}$)				Sb1	4*c*($\frac{1}{4}$,$\frac{1}{4}$,$\frac{1}{4}$)
					B (Å)^2	0.17(2)
Sb2	2*d*(0,0,$\frac{1}{2}$)				Sb2	4*b*(0,0,$\frac{1}{2}$)
					B (Å)^2	0.25(2)
O1	4*i*(0,y.z)				O1	4*e*(0,$\frac{1}{4}$,z)
y	0.311(2)	0.320(2)	0.329(1)	0.315(2)	*B* (Å)^2	0.49(5)
z	0.236(3)	0.219(3)	0.224(3)	0.205(2)	*z*	0.1553(2)
O2	4*i*(0,*y*.*z*)				O2	8*h*(0,*y*,*z*)
v	0.383(3)	0.386(1)	0.381(3)	0.392(1)	*y*	0.4064(2)
z	0.753(3)	0.752(2)	0.759(2)	0.752(2)	*z*	0.7284(2)
O22	4*i*(0,*y*,*z*)				*B* (Å)^2	0.56(5)
y	0.088(2)	0.092(3)	0.088(2)	0.086(2)		
z	0.725(4)	0.712(3)	0.712(3)	0.743(4)		
O3	8*j*(*x*,*y*,*z*)				O3	16*j*(*x*,*y*,*z*)
x	0.266(3)	0.272(2)	0.269(2)	0.263(2)	*x*	0.2079(1)
y	0.361(2)	0.358(1)	0.361(2)	0.3560(8)	*y*	0.3815(1)
z	0.454(2)	0.464(1)	0.461(2)	0.472(1)	*z*	0.4351(1)
O33	8*j*(*x*,*y*,*z*)				*B* (Å)^2	0.37(3)
x	0.209(2)	0.195(2)	0.192(1)	0.208(2)		
y	0.117(1)	0.111(2)	0.110(1)	0.120(1)		
z	0.423(1)	0.426(2)	0.423(2)	0.436(2)		
B (Å)^2	0.52(3)	0.37(6)	0.48(3)	0.77(4)		
R_{wp} (%)	3.05(11.13)	4.33(11.15)	3.06(10.81)	4.50(8.80)		3.78(9.60)
R_p (%)	2.26(8.11)	3.16(8.39)	2.33(8.18)	3.43(6.73)		2.85(7.30)
χ^2	2.28(1.98)	2.16(2.38)	2.12(2.35)	6.19(2.34)		2.82(1.79)

[a]The ratio between Ca and *Ln* is 1:1.
[b]Ca and Y are randomly distributed with the ratio 2:3.

[001], which is absent in $Ca_2Sb_2O_7$ due to the presence of a mirror plane perpendicular to [010], is large (18.0°). The latter tilting reduces the coordination of Ca(1) and the Ca(1)–O polyhedron is actually an octahedron. Between the Sb(1)O_6 rows lie rows of La(2)O_8 polyhedra, which are linked by common edges forming sheets perpendicular to [010]. The geometry of La(2)O_8 is a highly distorted square prism with the La–O bond distances ranging from 2.36 to 2.86 Å. The averaged value (2.58 Å) is, however, in good agreement with the sum of the corresponding ionic radii (2.54 Å) [21]. The randomly distributed (Ca/La)(11) atoms (Table 1) also coordinate with eight oxygens forming a deformed hexagonal bipyramid. The Sb(1)O_6, Sb(2)O_6 and (Ca/La)(22)O_6 octahedra form a three-dimensional framework. The O(2) atom has no Sb neighbours, which leads to short (*Ln* or Ca/*Ln*)–O(2) distances (Table 2).

Another way to view the weberite structure is based on the *fcc* close packing of the metal atoms with oxygens occupying the 7/8 available tetrahedral positions in between the metal layers (Fig. 3). In the parent weberite ($Ca_2Sb_2O_7$), there exist alternating Ca_3Sb and Sb_3Ca layers. As can clearly be seen, in $Ca_2La_3Sb_3O_{14}$ the Sb in the Ca_3Sb layer are replaced by Ca/La atoms, whereas the Sb atoms in the Sb_3Ca remain in the same positions.

The structures of $Ca_2Ln_3Sb_3O_{14}$ with *Ln* = Pr and Nd are similar to that of $Ca_2La_3Sb_3O_{14}$. For $Ca_2Y_3Sb_3O_{14}$, the distribution of Y and Ca is somewhat different. This can be seen from the relatively poor agreement factors (R_{wp} = 8.79 and 13.67% for neutron and X-ray data, respectively) when the structure of $Ca_2Y_3Sb_3O_{14}$ is modelled by using the same cation distributions found in $Ca_2La_3Sb_3O_{14}$. Particularly, the calculated X-ray intensities of some weak reflections, e.g. $2\theta \approx 17°$, 24°, 38.5°,

Table 2
Selected interatomic distances (Å) and angles (deg.) of $Ca_2Ln_3Sb_3O_{14}$ (*Ln* = La and Y) and $Ca_2Sb_2O_7$

$Ca_2La_3Sb_3O_{14}$		$Ca_2Y_3Sb_3O_{14}$		$Ca_2Sb_2O_7$	
Ca1–O22	2.29(2) × 2	(Ca/Y)1–O22	2.11(2) × 2	Ca1–O1	2.8044(7) × 2
Ca1–O3	2.34(3) × 4	(Ca/Y)1–O3	2.32(1) × 4	Ca1–O2	2.242(2) × 2
				Ca1–O3	2.500(1) × 4
(Ca/La)11–O1	2.70(2) × 2	(Ca/Y)11–O1	2.45(1) × 2		
(Ca/La)11–O2	2.24(2) × 2	(Ca/Y)11–O2	2.15(2) × 2		
(Ca/La)11–O33	2.60(1) × 4	(Ca/Y)11–O33	2.54(1) × 4		
La2–O2	2.36(1) × 2	(Ca/Y)2–O2	2.370(9) × 2	Ca2–O2	2.431(1) × 4
La2–O22	2.57(1) × 2	(Ca/Y)2–O22	2.52(1) × 2	Ca2–O3	2.725(1) × 4
La2–O3	2.54(1) × 2	(Ca/Y)2–O3	2.54(1) × 2		
La2–O33	2.86(1) × 2	(Ca/Y)2–O33	2.337(9) × 2		
(Ca/La)22–O1	2.84(2) × 2	(Ca/Y)22–O1	2.91(2) × 2		
(Ca/La)22–O2	2.29(1) × 2	(Ca/Y)22–O2	2.18(1) × 2		
(Ca/La)22–O3	2.53(1) × 4	(Ca/Y)22–O3	2.47(1) × 4		
Sb1–O1	2.004(7) × 2	Sb1–O1	2.000(6) × 2	Sb1–O1	1.9576(6) × 2
Sb1–O3	1.94(2) × 2	Sb1–O3	1.98(1) × 2	Sb1–O3	1.9514(10) × 4
Sb1–O33	1.96(1) × 2	Sb1–O33	1.96(1) × 2		
Sb2–O22	1.94(2) × 2	Sb2–O22	2.01(3) × 2	Sb2–O2	1.955(2) × 2
Sb2–O33	2.10(2) × 4	Sb2–O33	2.04(1) × 4	Sb2–O3	2.0008(9) × 4
Sb1–O1–Sb1	141(1)°		135.2(8)°	Sb1–O1–Sb1	137.6(1)°
Sb1–O33–Sb2	137.3(8)°		135.2(9)°	Sb1–O3–Sb2	135.04(5)°

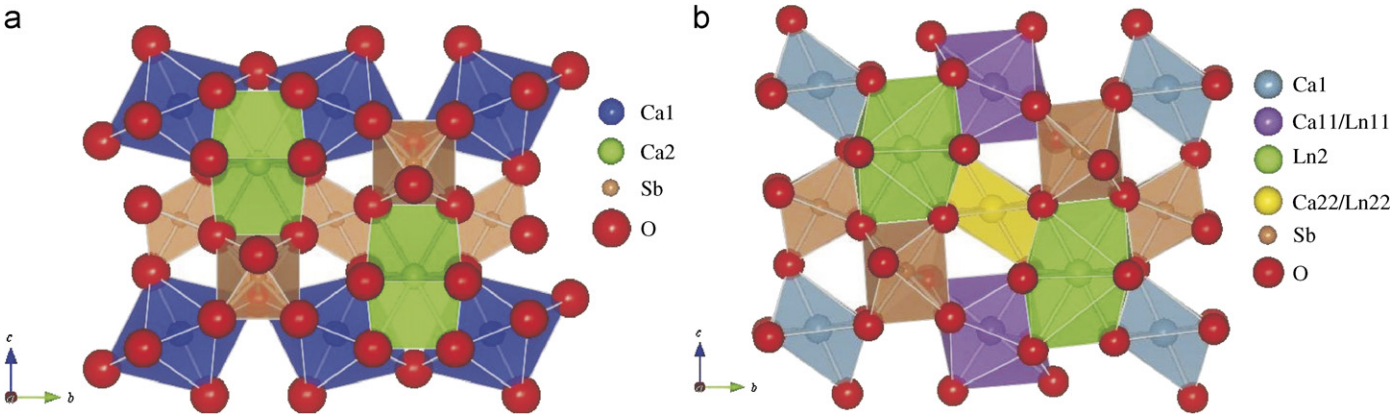

Fig. 2. Schematic representations of the crystal structures of $Ca_2Sb_2O_6$ (left) and $Ca_2La_3Sb_3O_{14}$ (right) showing the arrangement of metal–oxygen polyhedrons. Their structural differences are discussed in detail in the Section 4.

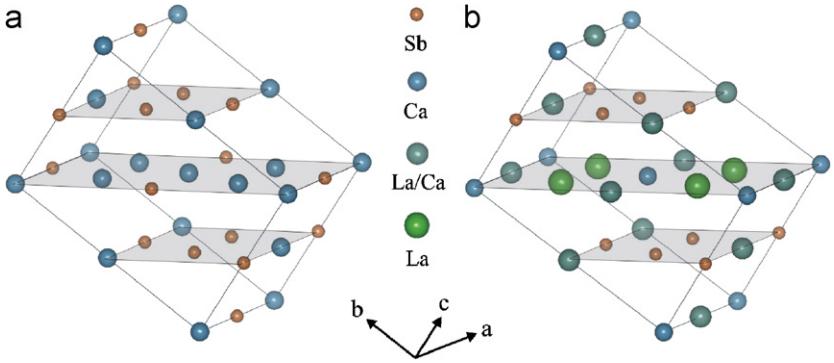

Fig. 3. Schematic drawing of the crystal structures of $Ca_2Sb_2O_6$ (left) and $Ca_2La_3Sb_3O_{14}$ (right) showing the *fcc* close packing of metal atoms. The oxygen atoms are omitted from the figure for clarity.

42.4° …, are much higher than the observed intensities. A model featuring the random distribution of Ca and Y over the positions 2*a*, 2*b*, 2*c* and 4*f* significantly improves the results of the refinement (Table 1).

The lattice constants of $Ca_2Ln_3Sb_3O_{14}$ with other lanthanides have been refined from the X-ray data (Table 3). The refinements indicate also that the ordering of Ca and *Ln* over the positions (0,0,0) and $(\frac{1}{4},\frac{1}{4},\frac{3}{4})$ gradually

Table 3
The lattice constants of some $Ca_2Ln_3Sb_3O_{14}$ as were refined from X-ray diffraction data

$Ca_2Ln_3Sb_3O_{14}$	a (Å)	b (Å)	c (Å)	α (deg.)
Sm	7.4664(2)	10.5409(3)	7.4445(2)	90.252(2)
Eu	7.4532(2)	10.5533(2)	7.4343(2)	90.173(2)
Gd	7.4376(2)	10.5187(3)	7.4290(2)	90.071(2)
Tb	7.42310(7)	10.4922(1)	7.41278(7)	90.0710(7)
Dy	7.4072(3)	10.4678(2)	7.3987(3)	90.042(3)
Yb	7.3534(4)	10.3960(5)	7.3499(2)	90.090(2)
Lu	7.3409(6)	10.3782(8)	7.3409(4)	89.928(4)

diminishes from Sm into a random structure in the case of $Ca_2Y_3Sb_3O_{14}$. Due to the high pseudo-symmetry and the limitations of the refinement program, exact refinement of the distribution of Ca and *Ln* over the four positions is not possible.

It is interesting to note that in $Ca_2Y_3Sb_3O_{14}$ the lattice parameters a and c are nearly equal and α is close to 90° (Table 1). In their X-ray diffraction study on $Ca_2Ln_3Sb_3O_{14}$, Burchard and Rüdorff [13] described the structure of $Ca_2Dy_3Sb_3O_{14}$ in the space group $P4/mnc$. However, inspecting the $h\,k\,l$ indices given by the authors has shown only a few very weak peaks, e.g. $d = 2.798$ Å indexed as (212), violating an I-centered lattice. As has been noticed before, the double perovskite-like Ca_2LnSbO_6 is sometimes present as an impurity phase and, coincidentally, the strongest reflections are very close to the d-spacing mentioned above. This is probably the reason why a primitive tetragonal unit cell has been found previously for $Ca_2Ln_3Sb_3O_{14}$ containing the smaller lanthanides [13]. Nevertheless, the chiolite structure ($Na_5Al_3F_{14}$) is not compatible with the title compounds despite the apparent resemblance of the stoichiometry. The chiolite structure consists of layers of AlF_6 along the [001] direction; but the similar SbO_6 layers in $Ca_2Ln_3Sb_3O_{14}$ are along the [101] direction. Since the cation distributions resemble each other, identification of the true structure based on the X-ray diffraction data only may be difficult. In this respect, neutron diffraction is better in determining the positions of oxygen atoms in the presence of heavy atoms.

It is worth mentioning that Burchard and Rüdorff [13] reported the compounds $Ca_2Ln_3Ta_3O_{14}$ (*Ln* = Dy, Y, Er, Yb) and $NaLn_4Sb_3O_{14}$ (*Ln* = Nd, Sm, Y, Er and Yb) as also adopting the chiolite structure. In the light of the present investigation, such a description may be incorrect. In fact, the lattice parameters reported for these compounds closely resemble those of $Ca_2Ln_3Sb_3O_{14}$. Our preliminary results indicate that $Ca_2Ln_3Ta_3O_{14}$ is likely to be a distorted weberite too.

A related but somewhat different structure has been observed in Na_2NiInF_7 [22]. This compound is a distorted weberite too, crystallizing in the space group *Pmnb*, which is a subgroup of *Imma*. In this structure In^{3+} occupies the 4*b* $(0,0,\frac{1}{2})$ position just as Al^{3+} does in the parent Na_2MgAlF_7. The octahedra are, however, tilted along two axes parallel to the [010] and [001] direction. Apparently, the stoichiometry of Na_2NiInF_7 does not need to split the cation positions, but the bigger In^{3+} does lower the symmetry of the parent weberite.

In conclusion, we have studied the structures of $Ca_2Ln_3Sb_3O_{14}$, together with $Ca_2Sb_2O_7$, and determined the crystal structure in the case of *Ln* = La, Pr, Nd and Y from the combined neutron and X-ray powder diffraction data. While $Ca_2Sb_2O_7$ is a normal weberite, $Ca_2Ln_3Sb_3O_{14}$ adopts the monoclinic space group $I2/m11$, representing a hitherto unknown type of deformation of the parent weberite structure. The earlier reported chiolite structure for $Ca_2Ln_3Sb_3O_{14}$ has not been found.

Acknowledgments

The authors are indebted to Mr. A. Bontenbal of NRG in Petten, The Netherlands, for the collection of the neutron diffraction data and to Dr. R.A.G. de Graaff for valuable discussions.

References

[1] A.F. Wells, Structural Inorganic Chemistry, Clarendon Press, Oxford, 1984.
[2] O. Knop, G. Demazeau, P. Hagenmuller, Can. J. Chem. 58 (1980) 2221.
[3] S.A. Ivanov, V.E. Zavodnik, Kristallografiya 35 (1990) 842.
[4] C. Jacoboni, A. Leble, J.J. Rousseau, J. Solid State Chem. 36 (1981) 297.
[5] E.H.P. Cordfunke, M.E. Huntelaar, D.J.W. IJdo, J. Solid State Chem. 146 (1999) 144.
[6] W.A. Groen, D.J.W. IJdo, Acta Crystallogr. C 44 (1988) 782.
[7] J. Reading, C.S. Knee, M.T. Weller, J. Mater. Chem. 12 (2002) 2376.
[8] E.H.P. Cordfunke, D.J.W. IJdo, J. Phys. Chem. Solids 49 (1988) 551.
[9] O. Knop, G. Demazeau, J. Solid State Chem. 39 (1981) 94.
[10] G. Desgardin, C. Robert, B. Raveau, Can. J. Chem. 54 (1976) 1665.
[11] G. Desgardin, C. Robert, B. Raveau, J. Inorg. Nucl. Chem. 39 (1977) 907.
[12] G. Burchard, W. Rüdorff, Z. Anorg. Allg. Chem. 454 (1979) 107.
[13] G. Burchard, W. Rüdorff, Z. Anorg. Allg. Chem. 445 (1978) 79.
[14] J. Sato, N. Saito, H. Nishiyama, Y. Inoue, J. Photochem. Photobiol. A 148 (2002) 85.
[15] X. Lin, F. Huang, W. Wang, Y. Wang, Y. Xia, J. Shi, Appl. Catal. A: General 313 (2006) 218.
[16] A. Byström, Ark. Kem. Miner. Geol. A 18 (1945) 8.
[17] C.J. Howard, B.A. Hunter, A Computer Program for Rietveld Analysis of X-ray and Neutron Powder Diffraction Patterns, Lucas Height Research Laboratories, 1998.
[18] R.B. Von Dreele, in: R.A. Young (Ed.), The Rietveld Method, Oxford University Press, Oxford, 1993 (chapter 12).
[19] A. Byström, Ark. Kem. Miner. Geol. 18 (1945) 10.
[20] M. Renninger, Z. Phys. 106 (1937) 141.
[21] R.D. Shannon, Acta Crystallogr. A 32 (1976) 751.
[22] G. Frenzen, W. Massa, D. Babel, N. Ruchaud, J. Grannec, A. Tressaud, P. Hagenmuller, J. Solid State Chem. 98 (1992) 121.